

Self-Reinforcing Prototype Evolution with Dual-Knowledge Cooperation for Semi-Supervised Lifelong Person Re-Identification

Supplementary Material

In our supplementary materials, we provide additional implementation details for the proposed approach and the Semi-LReID benchmark. Furthermore, we include extensive quantitative and qualitative results that emphasize the effectiveness of our method in comparison to existing works.

In summary, the supplementary materials primarily include:

- Detailed implementation and architecture of the proposed distribution alignment network (DANet).
- Ablation studies on the components of the DKCP module.
- Pseudo-code of our SPRED method.
- Overview of the ReID datasets and their arrangement in the proposed Semi-LReID benchmark.
- Quantitative comparisons with state-of-the-art methods under different dataset orders.
- Quantitative comparisons with state-of-the-art methods at a label rate of $r=100\%$.
- Quantitative comparisons with state-of-the-art NoisyLReID and SLL methods.
- Qualitative results on the feature distribution and label prediction accuracy.

1. Implementation of Distribution Alignment Network

Inspired by [4], which revealed that the primary distribution difference across ReID datasets lies in color styles, we propose a distribution alignment network (DANet) based on the architecture of [4].

As illustrated in Fig. 1, for a given image x , the channel-wise mean and variance are calculated, *i.e.*, (μ_R, σ_R) , (μ_G, σ_G) , and (μ_B, σ_B) . These statistics are modeled as Gaussian distributions per channel. For example, the R -channel mean and standard deviation follow $\mathcal{N}(\mu_R, \sigma_R^2)$ and $\mathcal{N}(\sigma_R, \sigma_R^2)$, respectively. Next, the color augmentation is conducted which involves sampling new mean and standard deviation values for each channel. For instance, for the R -channel, given a sampled mean $\dot{\mu}_R$ and standard deviation $\dot{\sigma}_R$, the augmented image \dot{x}_R is computed as:

$$\dot{x}_R = (x_R - \mu_R + \dot{\mu}_R) \frac{\dot{\sigma}_R}{\sigma_R} \quad (1)$$

Similarly, the augmented G channel \dot{x}_G and B channel \dot{x}_B are generated, forming the final augmented image \dot{x} .

Then, we introduce a lightweight distribution alignment network (DANet) Θ_t which contains a MobileNet [6] backbone and a convolutional decoder. Θ_t generates a recon-

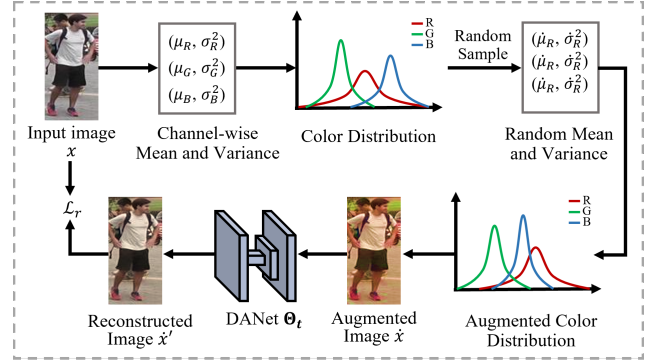


Figure 1. Training process of distribution alignment network (DANet)

structed image \hat{x}' from \hat{x} . The reconstruction process is guided by a mean absolute error (MAE) loss \mathcal{L}_r , defined as:

$$\mathcal{L}_r = \|x - \hat{x}'\| \quad (2)$$

Different from [4], which employed additional LBP transformations and formed a multi-step process for reconstruction during testing, our approach performs input-wise augmentation and direct reconstruction. This ensures an efficient end-to-end workflow, significantly simplifying applications while maintaining robust alignment.

Note that during the t -th ($t > 1$) training step, the previous DANet Θ_{t-1} is utilized to improve the adaptation of old knowledge to the new dataset D_t . Additionally, Θ_{t-1} only needs to forward once for each image, and the generated clustering results from the Old Knowledge Aligning-based Clustering (OKAC) strategy can be reused across training epochs, ensuring computational efficiency.

To verify the effectiveness of distribution alignment, we conduct an ablation study in Tab. 1. The results show that when introducing Θ_{t-1} , consistent **0.6%-1.0%** improvement on Seen-Avg and UnSeen-Avg performance is achieved in our framework.

2. Ablation Studies on DKCP

Our Dual-Knowledge Cooperation-driven Pseudo-label Purification (DKCP) module is designed to filter noisy pseudo-labels by leveraging both old and new model knowledge. To achieve this, two complementary strategies are introduced: Old Knowledge Aligning-based Clustering (OKAC) and

New Knowledge Clustering (NKC), which extract knowledge from the old and new models, respectively.

To verify the effectiveness of our dual-knowledge utilization, we conduct ablation studies as summarized in Tab. 2. Starting from the DPL+NPL without DKCP, we progressively incorporate OKAC and NKC. The results demonstrate that integrating either OKAC or NKC individually improves Semi-LReID performance. This improvement occurs because prototype-based pseudo-label generation primarily focuses on prototype-instance relations, neglecting inter-instance relations. By contrast, OKAC and NKC extract inter-instance relations through clustering, complementing the prototype-based pseudo-label generation. When both OKAC and NKC are utilized together, the performance is further enhanced. This advancement arises from our method effectively combining the generalizable old knowledge and abundant new knowledge, leading to the generation of higher-quality pseudo-labels.

| Method | Seen-Avg | | UnSeen-Avg | |
|----------------------------------|-------------|-------------|-------------|-------------|
| | mAP | R@1 | mAP | R@1 |
| Ours (w/o DANet Θ_{t-1}) | 42.5 | 53.8 | 51.1 | 43.6 |
| Ours (w/ DANet Θ_{t-1}) | 43.2 | 54.4 | 51.7 | 44.6 |

Table 1. Ablation study on DANet Θ_{t-1} .

| DPL+NPL | OKAC | NKC | Seen-Avg | | UnSeen-Avg | |
|---------|------|-----|-------------|-------------|-------------|-------------|
| | | | mAP | R@1 | mAP | R@1 |
| ✓ | | | 38.0 | 49.8 | 47.4 | 40.5 |
| ✓ | ✓ | | 39.6 | 51.2 | 48.3 | 42.8 |
| ✓ | | ✓ | 40.1 | 51.4 | 47.6 | 41.0 |
| ✓ | ✓ | ✓ | 43.2 | 54.4 | 51.7 | 44.6 |

Table 2. Ablation study on components of DKCP. ‘DPL+NPL’ represents our method without DKCP.

3. Algorithm

The pseudo-code of our SPRED method is shown in Alg 1.

4. Datasets Details of Semi-LReID Benchmark

We establish the Semi-LReID benchmark based on the existing LReID configuration[12], incorporating 12 widely-used ReID datasets: Market1501 [25], LPW [15], CUHK-SYSU [19], MSMT17-V2 [17], CUHK03 [10], CUHK01 [9], CUHK02 [8], VIPeR [3], PRID [5], iLIDS [1], GRID [11], and SenseReID [24]). The detailed dataset statistics are presented in Tab. 3. Among these datasets, CUHK-SYSU is initially proposed for the person search. To adapt it for ReID, we crop individual-level images using the ground-truth bounding box annotations.

Algorithm 1 SPRED Algorithm

Input: $D_t = \{(X_t^l, Y_t^l)\} \cup \{X_t^u\}$, M_{t-1} , $\mathcal{P}_{t-1} = \{p_{t-1}^i\}_{i=1}^{L_{t-1}}$.

Output: $M_t, \mathcal{P}_t = \{p_t^i\}_{i=1}^{L_t}$

Old Knowledge Aligning-based Clustering

$D_t^* = \text{DANet}(D_t)$; *# Apply style transfer*

$F_{t-1}^* = M_{t-1}(D_t^*)$; *# Extract feature*

$\mathcal{C}_{t-1} = \{C_1^{t-1}, C_2^{t-1}, \dots, C_{N_C}^{t-1}\}$; *# Apply clustering*

Initialize $M_t^0 = M_{t-1}$

for $e = 1$ **to** N_{epoch} **do**

Neighbor Prototype Labeling

for x **in** X_t^u **do**

$f_t^{e-1} = M_t^{e-1}(x)$;

Obtain top-2 nearest prototypes p_A and p_B ;

$s_A = \frac{e^{<f_t^{e-1}, p_A>}}{e^{<f_t^{e-1}, p_A>} + e^{<f_t^{e-1}, p_B>}}$; *#Classification score*

Obtain l_i according to Eq. (6);

end for

New Knowledge Clustering

$F_t^{e-1} = M_t^{e-1}(D_t)$; *# Extract feature*

$\mathcal{C}_t^{e-1} = \{C_1^{e-1}, C_2^{e-1}, \dots, C_{N_C}^{e-1}\}$; *# Clustering*

$Y_t^{pse} = Y_{t-1}^{pse} \cup Y_{e-1}^{pse}$;

Noisy Pseudo-Label Filtering

Obtain $Y_{e-1}^{pse} = \{y_{i,e-1}^{pse} : x_i \in X_t^u\}$ according to

$LC_s(x_i, \mathcal{S}^{e-1}, \mathcal{C}_t^{e-1})$;

Obtain $Y_{t-1}^{pse} = \{y_{i,t-1}^{pse} : x_i \in X_t^u\}$ according to

$LC_s(x_i, \mathcal{S}^{e-1}, \mathcal{C}_{t-1})$;

Dynamic Prototype-guided LReID Learning

for (x, y) **in** (X_t^{pse}, Y_t^{pse}) **do**

$\mathcal{L}_{base} = \mathcal{L}_p + \mathcal{L}_{Tri}$,

$\mathcal{L}_s = \mathcal{L}_{KL}(S(f_{t-1}^e, \mathcal{P}_{t-1}) || S(f_t^e, \mathcal{P}_{t-1}))$;

Optimize M_t^e with loss $\mathcal{L} = \mathcal{L}_{base} + \alpha \mathcal{L}_s$;

end for

end for

$M_t = \delta_t M_{t-1} + (1 - \delta_t) M_t^{N_{epoch}}$; *# δ_t is obtained according to LSTKC [22]*

Return $M_t, \mathcal{P}_t = \{p_t^i\}_{i=1}^{L_t}$;

Then, a subset where each identity has at least 4 bounding boxes is selected following [12]. Additionally, LPW [15], originally a video-based person re-identification dataset, is transformed into a ReID dataset by sampling one frame every 15 frames from the original sequences. The resulting dataset is then structured in accordance with the Mar-

| Type | Datasets Name | Original Identities | | | Semi-LReID Identities | | |
|--------|------------------|---------------------|-------|---------|-----------------------|-------|---------|
| | | Train | Query | Gallery | Train | Query | Gallery |
| Seen | CUHK03 [10] | 767 | 700 | 700 | 500 | 700 | 700 |
| | Market-1501 [25] | 751 | 750 | 751 | 500 | 751 | 751 |
| | LPW [15] | 875 | 876 | 876 | 500 | 876 | 876 |
| | CUHK-SYSU [19] | 942 | 2900 | 2900 | 500 | 2900 | 2900 |
| | MSMT17-V2 [17] | 1041 | 3060 | 3060 | 500 | 3060 | 3060 |
| Unseen | i-LIDS [1] | 243 | 60 | 60 | - | 60 | 60 |
| | VIPR [3] | 316 | 316 | 316 | - | 316 | 316 |
| | GRID [11] | 125 | 125 | 126 | - | 125 | 126 |
| | PRID [5] | 100 | 100 | 649 | - | 100 | 649 |
| | CUHK01 [9] | 485 | 486 | 486 | - | 486 | 486 |
| | CUHK02 [8] | 1677 | 239 | 239 | - | 239 | 239 |
| | SenseReID [24] | 1718 | 521 | 1718 | - | 521 | 1718 |

Table 3. The statistics of datasets used in the Semi-LReID benchmark. ‘-’ indicates the dataset is only used as a test domain.

ket1501 [25] format. In addition, to mitigate the data imbalance between datasets [12, 13], 500 identities of each dataset are selected to form the Semi-LReID benchmark. In Tab. 3, the column ‘Original Identities’ represents the total number of identities in each dataset, while ‘Semi-LReID Identities’ lists the selected identities for our benchmark. To generate training data under different label rates, we ensure that each identity includes at least two labeled samples. Random selection is then applied to the remaining data until the predefined label rate is satisfied.

5. Experimental Results on Different Dataset Orders

In our main paper, the default training dataset order follows Market-1501→CUHK-SYSU→LPW→MSMT17→CUHK03, denoted as Training Order-1¹. In this section, we extend the evaluation by comparing our method with existing approaches under another training order: LPW→MSMT17→Market-1501→CUHK-SYSU→CUHK03, referred to as Training Order-2². The results are summarized in Tab. 4.

Compared with LReID Methods: Under Training Order-2, our proposed SPRED consistently surpasses existing LReID methods in both Seen-Avg and UnSeen-Avg mAP/R@1 across different label rates. Specifically, compared to the state-of-the-art LSTKC, SPRED achieves increasing improvements of **2.6%/2.2%**, **9.2%/9.7%**, and **14.4%/16.1%** in Seen-Avg mAP/R@1 as the label rate drops from 50% to 10%. Besides, SPRED obtains **1.9%/1.9%**, **8.0%/7.5%**, and **11.8%/11.4%** improvements in UnSeen-Avg mAP/R@1. These results highlight

¹(Training Order-1) Market-1501→CUHK-SYSU→LPW → MSMT17→CUHK03

²(Training Order-2) LPW→MSMT17→Market-1501→ CUHK-SYSU →CUHK03

SPRED’s superior adaptability to scenarios with reduced labeling rates, outperforming current state-of-the-art LReID methods in low-labeling regimes.

Compared with SSL+LReID Methods: When adopting the traditional data augmentation configuration, our SPRED model demonstrates significantly superior performance, particularly at a low label rate of $r=10\%$. When integrating the data augmentation strategy from SSL, the enhanced SPRED[‡] model outperforms all existing methods in both Seen-Avg mAP/R@1 and UnSeen-Avg mAP/R@1 metrics across all label rates. Specifically, SPRED[‡] achieves notable improvements in Seen-Avg mAP/R@1 of **2.9%/2.2%**, **9.3%/10.2%** and **13.3%/13.8%** at label rates of 50%, 20%, and 10%, respectively. In addition, in UnSeen-Avg mAP/R@1, improvements of **3.4%/3.2%**, **6.5%/6.0%** and **9.8%/9.4%** are observed at label rates of 50%, 20%, and 10%, separately. These results underscore the effectiveness of our neighbor prototype labeling and dual-knowledge utilization mechanisms, which significantly enhance pseudo-label quality and improve the model’s capability to acquire new knowledge.

6. Experimental Results Under Label Rate $r=100\%$

We also evaluate our method under the fully-labeled scenario, where the label rate $r=100\%$. As shown in Tab. 5, our SPRED achieves competitive results with the latest LReID methods across both training orders. Additionally, the enhanced SPRED[‡] surpasses all existing methods with significant margins. Specifically, SPRED[‡] outperforms the state-of-the-art DKP by **4.6%/5.4%** and **2.0%/3.4%** in Seen-Avg mAP/R@1 across the two training orders. For UnSeen-Avg mAP/R@1, SPRED[‡] achieves improvements of **4.1%/5.1%** and **1.3%/1.2%** over DKP. These results verify the adaptability of our method to varying scenarios.

| r | Type | Method | LPW | | MSMT17 | | Market-1501 | | CUHK-SYSU | | CUHK03 | | Seen-Avg | | UnSeen-Avg | | |
|------------|------------|---------------------------|--------------|------|--------|------|-------------|------|-----------|------|--------|------|-------------|-------------|-------------|-------------|------|
| | | | mAP | R@1 | mAP | R@1 | mAP | R@1 | mAP | R@1 | mAP | R@1 | mAP | R@1 | mAP | R@1 | |
| 50% | LReID | PatchKD [16] | 45.6 | 57.6 | 4.2 | 11.9 | 34.4 | 58.7 | 70.6 | 74.0 | 19.5 | 19.6 | 34.9 | 44.4 | 38.5 | 33.4 | |
| | | DKP [21] | 41.0 | 53.2 | 12.2 | 29.8 | 49.8 | 72.7 | 81.5 | 83.7 | 27.7 | 26.9 | 42.4 | 53.3 | 53.8 | 46.9 | |
| | | LSTKC [22] | 37.2 | 48.7 | 13.1 | 31.8 | 51.9 | 73.4 | 81.1 | 83.2 | 37.9 | 37.9 | 44.2 | 55.0 | 53.3 | 46.0 | |
| | SSL+LReID | CDMAD [†] [7] | 30.4 | 45.7 | 6.9 | 22.5 | 27.9 | 57.5 | 76.2 | 79.8 | 11.9 | 11.0 | 30.7 | 43.3 | 46.8 | 40.7 | |
| | | ShrinkM [†] [23] | 40.3 | 54.8 | 18.8 | 44.8 | 53.5 | 77.0 | 77.5 | 79.7 | 36.4 | 36.8 | 45.3 | 58.6 | 57.7 | 50.9 | |
| | | SimMV2 [†] [26] | 27.3 | 39.0 | 8.7 | 25.3 | 42.4 | 66.8 | 63.0 | 66.1 | 29.7 | 32.4 | 34.2 | 45.9 | 44.8 | 38.0 | |
| | | DPIS [†] [14] | 38.4 | 50.4 | 13.4 | 31.7 | 52.1 | 74.2 | 82.0 | 84.0 | 35.8 | 36.6 | 44.3 | 55.4 | 53.7 | 46.6 | |
| | | HDC [†] [18] | 41.1 | 54.2 | 18.5 | 43.6 | 55.0 | 77.9 | 81.0 | 83.2 | 40.2 | 41.4 | 47.2 | 60.1 | 57.0 | 50.3 | |
| | Ours | SPRED | 48.8 | 60.4 | 10.6 | 26.4 | 50.5 | 72.3 | 82.4 | 84.1 | 41.9 | 42.6 | 46.8 | 57.2 | 55.2 | 47.9 | |
| | | SPRED[‡] | 47.2 | 60.0 | 16.8 | 40.9 | 57.8 | 78.4 | 80.4 | 82.2 | 48.2 | 49.9 | 50.1 | 62.3 | 61.1 | 54.1 | |
| | 20% | LReID | PatchKD [16] | 28.2 | 37.4 | 2.6 | 7.3 | 20.1 | 40.7 | 66.3 | 70.5 | 5.8 | 4.7 | 24.6 | 32.1 | 27.9 | 23.1 |
| | | | DKP [21] | 21.7 | 31.5 | 7.2 | 21.3 | 28.0 | 51.6 | 73.8 | 76.7 | 6.7 | 5.5 | 27.5 | 37.3 | 40.0 | 33.3 |
| LSTKC [22] | | | 24.3 | 33.8 | 9.3 | 23.8 | 39.5 | 62.6 | 76.7 | 79.6 | 18.7 | 17.3 | 33.7 | 43.4 | 44.3 | 37.2 | |
| SSL+LReID | | CDMAD [†] [7] | 20.7 | 32.7 | 5.8 | 19.5 | 26.3 | 53.6 | 73.6 | 77.6 | 9.1 | 7.4 | 27.1 | 38.2 | 43.5 | 37.8 | |
| | | ShrinkM [†] [23] | 31.9 | 45.8 | 15.1 | 38.9 | 44.6 | 70.4 | 73.6 | 76.6 | 23.3 | 22.9 | 37.7 | 50.9 | 51.2 | 44.5 | |
| | | SimMV2 [†] [26] | 26.6 | 38.8 | 10.4 | 28.3 | 39.3 | 62.5 | 67.5 | 69.9 | 19.1 | 18.4 | 32.6 | 43.6 | 46.4 | 38.7 | |
| | | DPIS [†] [14] | 25.1 | 35.9 | 9.7 | 25.0 | 41.0 | 64.1 | 78.7 | 81.5 | 19.2 | 17.3 | 34.7 | 44.8 | 46.1 | 39.1 | |
| | | HDC [†] [18] | 28.6 | 41.1 | 12.4 | 32.6 | 43.5 | 66.9 | 76.0 | 78.5 | 24.3 | 23.9 | 37.0 | 48.6 | 50.1 | 42.3 | |
| Ours | | SPRED | 44.8 | 56.3 | 9.6 | 24.1 | 47.0 | 69.0 | 82.1 | 84.1 | 31.1 | 32.2 | 42.9 | 53.1 | 52.3 | 44.7 | |
| | | SPRED[‡] | 42.2 | 55.5 | 16.2 | 40.7 | 54.3 | 76.7 | 78.7 | 80.6 | 40.3 | 40.5 | 46.3 | 58.8 | 57.7 | 50.5 | |
| 10% | | LReID | PatchKD [16] | 15.6 | 22.8 | 1.4 | 4.2 | 12.0 | 28.9 | 61.8 | 65.4 | 4.0 | 3.2 | 19.0 | 24.9 | 22.5 | 18.1 |
| | | | DKP [21] | 12.5 | 19.4 | 5.1 | 15.4 | 18.7 | 40.2 | 69.2 | 72.3 | 5.0 | 3.8 | 22.1 | 30.2 | 34.6 | 28.5 |
| | LSTKC [22] | | 17.4 | 24.9 | 6.3 | 17.1 | 27.3 | 49.6 | 73.1 | 76.0 | 13.6 | 11.1 | 27.5 | 35.7 | 38.9 | 32.0 | |
| | SSL+LReID | CDMAD [†] [7] | 17.8 | 28.9 | 6.0 | 20.2 | 25.9 | 52.6 | 72.0 | 75.6 | 9.3 | 7.8 | 26.2 | 37.0 | 41.7 | 35.0 | |
| | | ShrinkM [†] [23] | 24.8 | 37.8 | 11.7 | 32.2 | 33.9 | 59.6 | 71.0 | 73.9 | 19.1 | 18.6 | 32.1 | 44.4 | 46.9 | 39.6 | |
| | | SimMV2 [†] [26] | 22.4 | 33.2 | 8.3 | 23.6 | 31.0 | 53.9 | 65.7 | 69.2 | 14.7 | 14.3 | 28.4 | 38.8 | 42.1 | 34.7 | |
| | | DPIS [†] [14] | 17.7 | 26.1 | 6.2 | 17.0 | 28.5 | 51.1 | 74.1 | 77.2 | 14.1 | 12.4 | 28.1 | 36.8 | 40.7 | 33.4 | |
| | | HDC [†] [18] | 17.5 | 25.7 | 5.7 | 17.8 | 26.0 | 48.8 | 71.5 | 75.0 | 13.4 | 11.7 | 26.8 | 35.8 | 41.3 | 34.1 | |
| | Ours | SPRED | 36.3 | 47.3 | 9.9 | 24.9 | 47.4 | 68.6 | 81.3 | 83.2 | 34.8 | 34.9 | 41.9 | 51.8 | 50.7 | 43.4 | |
| | | SPRED[‡] | 40.6 | 54.1 | 16.3 | 40.3 | 52.9 | 76.1 | 78.5 | 81.2 | 38.6 | 39.2 | 45.4 | 58.2 | 56.7 | 49.0 | |

Table 4. Results comparison under different label rate r under Training Order-2: LPW→MSMT17→Market-1501→CUHK-SYSU→CUHK03. [†] indicates the state-of-the-art SSL method is integrated with the anti-forgetting designs of LSTKC. [‡] represents adopting the data augmentation strategy of ShrinkM.

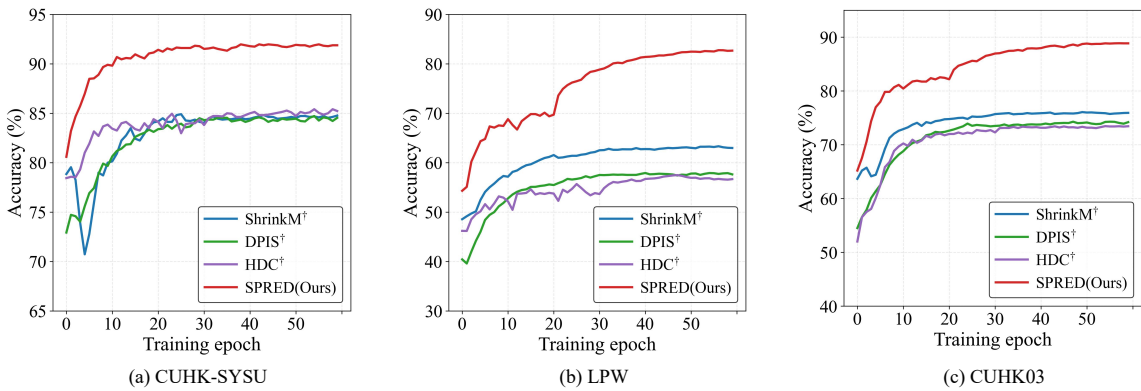


Figure 2. Label prediction accuracy of different methods. The compared methods are trained on Training Order-1 with label rate $r=10\%$

| r | Method | Publication | Market-1501 | | CUHK-SYSU | | LPW | | MSMT17 | | CUHK03 | | Seen-Avg | | UnSeen-Avg | |
|------|--------------------------|-------------|-------------|------|-----------|------|------|------|--------|------|--------|------|-------------|-------------|-------------|-------------|
| | | | mAP | R@1 | mAP | R@1 | mAP | R@1 | mAP | R@1 | mAP | R@1 | mAP | R@1 | mAP | R@1 |
| 100% | PatchKD | MM'22 | 71.6 | 87.7 | 77.0 | 79.6 | 33.2 | 41.9 | 7.0 | 18.5 | 29.5 | 30.4 | 43.7 | 51.6 | 47.8 | 41.4 |
| | LSTKC | AAAI'24 | 57.0 | 78.6 | 82.9 | 84.9 | 47.2 | 58.4 | 18.4 | 41.1 | 42.3 | 43.7 | 49.6 | 61.3 | 57.8 | 50.2 |
| | DKP | CVPR'24 | 60.0 | 80.3 | 84.1 | 85.9 | 46.0 | 57.9 | 17.7 | 38.5 | 41.0 | 41.4 | 49.8 | 60.8 | 57.5 | 50.7 |
| | SPRED | This Paper | 63.1 | 81.7 | 83.2 | 84.8 | 50.6 | 60.7 | 15.2 | 34.5 | 48.6 | 50.0 | 52.1 | 62.3 | 58.7 | 50.7 |
| | SPRED[‡] | This Paper | 65.0 | 83.3 | 81.8 | 83.6 | 51.1 | 63.1 | 21.4 | 47.5 | 52.6 | 53.6 | 54.4 | 66.2 | 62.8 | 55.8 |

| r | Method | Publication | LPW | | MSMT17 | | Market-1501 | | CUHK-SYSU | | CUHK03 | | Seen-Avg | | UnSeen-Avg | |
|------|--------------------------|-------------|------|------|--------|------|-------------|------|-----------|------|--------|------|-------------|-------------|-------------|-------------|
| | | | mAP | R@1 | mAP | R@1 | mAP | R@1 | mAP | R@1 | mAP | R@1 | mAP | R@1 | mAP | R@1 |
| 100% | PatchKD | MM 2022 | 58.0 | 69.0 | 6.3 | 16.7 | 46.3 | 70.6 | 75.7 | 78.5 | 29.6 | 30.2 | 43.2 | 53.0 | 45.3 | 38.5 |
| | LSTKC | AAAI 2024 | 46.7 | 57.6 | 14.9 | 33.9 | 56.5 | 78.0 | 84.0 | 86.1 | 42.1 | 43.7 | 48.8 | 59.9 | 57.4 | 49.5 |
| | DKP | CVPR 2024 | 49.5 | 61.4 | 14.1 | 32.6 | 60.3 | 80.6 | 84.5 | 86.4 | 43.6 | 43.7 | 50.4 | 60.9 | 59.5 | 52.4 |
| | SPRED | This Paper | 51.8 | 62.4 | 10.4 | 26.2 | 56.8 | 77.0 | 84.5 | 85.9 | 42.9 | 43.8 | 49.3 | 59.1 | 57.1 | 49.1 |
| | SPRED[‡] | This Paper | 51.6 | 63.4 | 16.4 | 40.1 | 61.9 | 82.5 | 82.7 | 84.4 | 49.4 | 51.0 | 52.4 | 64.3 | 60.8 | 53.6 |

Table 5. Comparison with LReID methods under label rate $r=100%$ on Training Order-1: Market-1501→CUHK-SYSU→LPW→MSMT17→CUHK03 and Training Order-2: LPW→MSMT17→Market-1501→CUHK-SYSU→CUHK03.

| r | Method | Publication | Market-1501 | | CUHK-SYSU | | LPW | | MSMT17 | | CUHK03 | | Seen-Avg | | UnSeen-Avg | |
|-----|--------------------------|-------------|-------------|------|-----------|------|------|------|--------|------|--------|------|-------------|-------------|-------------|-------------|
| | | | mAP | R@1 | mAP | R@1 | mAP | R@1 | mAP | R@1 | mAP | R@1 | mAP | R@1 | mAP | R@1 |
| 50% | CKP | MM'24 | 55.2 | 78.5 | 81.0 | 82.8 | 44.3 | 56.9 | 17.6 | 40.5 | 39.2 | 40.9 | 47.4 | 59.9 | 55.7 | 48.1 |
| | LDC | ECCV'24 | 23.4 | 50.1 | 61.1 | 65.9 | 19.3 | 32.7 | 8.8 | 29.4 | 17.7 | 17.8 | 26.0 | 39.2 | 38.7 | 32.3 |
| | SPRED | This Paper | 59.8 | 79.7 | 82.8 | 84.6 | 49.7 | 60.2 | 17.4 | 38.2 | 40.6 | 41.3 | 50.1 | 60.8 | 57.8 | 50.3 |
| | SPRED[‡] | This Paper | 59.4 | 80.7 | 79.6 | 81.5 | 47.3 | 60.2 | 21.6 | 47.3 | 48.4 | 49.4 | 51.3 | 63.8 | 60.7 | 53.9 |
| 20% | CKP | MM'24 | 48.1 | 72.7 | 78.8 | 81.4 | 39.2 | 53.4 | 16.2 | 38.5 | 29.7 | 29.4 | 42.4 | 55.1 | 52.2 | 43.8 |
| | LDC | ECCV'24 | 19.1 | 44.8 | 56.0 | 60.8 | 15.0 | 26.6 | 6.5 | 23.1 | 8.2 | 6.8 | 21.0 | 32.4 | 32.3 | 26.5 |
| | SPRED | This Paper | 54.7 | 75.7 | 81.1 | 83.0 | 45.0 | 56.9 | 16.1 | 36.3 | 35.8 | 35.4 | 46.5 | 57.5 | 55.7 | 48.4 |
| | SPRED[‡] | This Paper | 54.6 | 77.1 | 78.5 | 80.5 | 44.9 | 58.9 | 21.3 | 47.5 | 38.6 | 38.2 | 47.6 | 60.4 | 58.9 | 51.5 |
| 10% | CKP | MM'24 | 40.4 | 67.0 | 75.3 | 78.3 | 33.2 | 46.2 | 13.5 | 34.5 | 24.3 | 24.2 | 37.3 | 50.0 | 47.9 | 40.8 |
| | LDC | ECCV'24 | 12.3 | 33.3 | 52.4 | 56.6 | 8.9 | 16.8 | 3.9 | 16.0 | 5.6 | 5.1 | 16.6 | 25.5 | 28.4 | 22.6 |
| | SPRED | This Paper | 45.9 | 69.4 | 79.3 | 81.6 | 40.0 | 51.1 | 14.2 | 33.0 | 36.7 | 37.1 | 43.2 | 54.4 | 51.7 | 44.6 |
| | SPRED[‡] | This Paper | 49.5 | 74.0 | 76.5 | 79.1 | 40.9 | 55.4 | 19.4 | 45.3 | 37.5 | 38.4 | 44.8 | 58.4 | 55.9 | 48.7 |

Table 6. Comparison with NoisyLReID and SSLL methods on Training Order-1: Market-1501→CUHK-SYSU→LPW→MSMT17→CUHK03.

Note that while DKP [21] outperforms our SPRED at the label rate of 100% under training order-2 due to its distribution modeling design, this approach relies heavily on abundant labels to ensure reliable identity distribution modeling. In scenarios with insufficient labeled samples, the learned distributions become less reliable, leading to degraded performance, as demonstrated in Tab. 4. Consequently, our method is more suitable in situations where the labeling source is restricted.

7. Quantitative comparisons with state-of-the-art NoisyLReID and SSLL methods

We also compare our proposed method with the latest Noisy Lifelong Person Re-Identification (NoisyLReID) method CKP [20] by assigning all the unlabeled data with the same label, serving as noisy data. Besides, the exemplar-free

SSLL method LDC [2] is also compared (with sequential fine-tune as the baseline). The results in Tab. 6 show that our SPRED and SPRED[‡] outperform both competitors significantly across all label rates.

8. Additional Visualization on Prediction and Features

More Identity Prediction Capacity Visualization. Beyond the prediction accuracy curves presented in the main paper, we provide additional visualizations for CUHK-SYSU, LPW, and CUHK03 datasets in Fig. 2. The results show that SPRED consistently achieves higher prediction accuracy throughout training epochs. This can be attributed to the cyclically evolved pseudo-labeling mechanism, where pseudo-label prediction and purification iteratively reinforce each other.

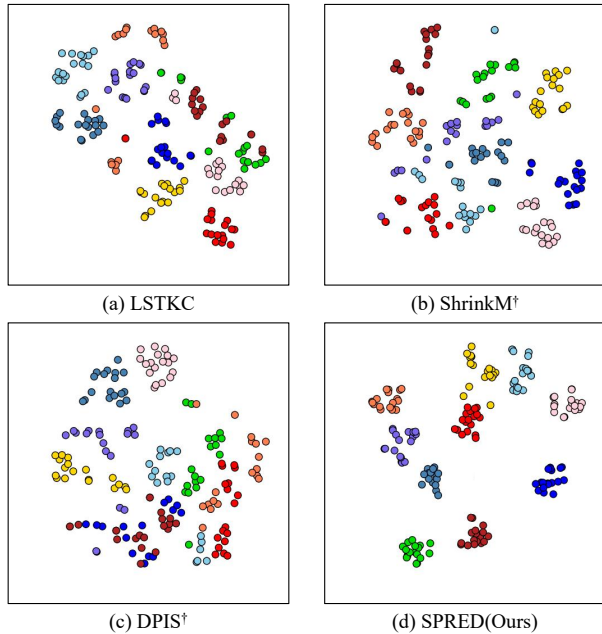


Figure 3. Visualization of test feature distribution. The compared methods are trained on Training Order-1 with label rate $r=10\%$. Each color represents an identity.

Testing Feature Visualization. We visualize the test data features in Fig. 3, where each point represents the feature of a test sample, with each color representing an identity. The results illustrate that features extracted by SPRED exhibit better clustering compared to existing methods. This improvement arises from the dual-knowledge-guided pseudo-label purification mechanism, which enhances pseudo-label quality and facilitates effective knowledge learning.

References

- [1] Home Office Scientific Development Branch. Imagery library for intelligent detection systems (i-lids). In *2006 IET conference on crime and security*, pages 445–448. IET, 2006. 2, 3
- [2] Alex Gomez-Villa, Dipam Goswami, Kai Wang, Andrew D Bagdanov, Bartłomiej Twardowski, and Joost van de Weijer. Exemplar-free continual representation learning via learnable drift compensation. In *ECCV*, pages 473–490. Springer, 2024. 5
- [3] Douglas Gray and Hai Tao. Viewpoint invariant pedestrian recognition with an ensemble of localized features. In *ECCV*, pages 262–275. Springer, 2008. 2, 3
- [4] Jianyang Gu, Hao Luo, Kai Wang, Wei Jiang, Yang You, and Jian Zhao. Color prompting for data-free continual unsupervised domain adaptive person re-identification. *arXiv preprint arXiv:2308.10716*, 2023. 1
- [5] Martin Hirzer, Csaba Beleznai, Peter M Roth, and Horst Bischof. Person re-identification by descriptive and discriminative classification. In *Image Analysis*, pages 91–102. Springer, 2011. 2, 3
- [6] Andrew Howard, Mark Sandler, Grace Chu, Liang-Chieh Chen, Bo Chen, Mingxing Tan, Weijun Wang, Yukun Zhu, Ruoming Pang, Vijay Vasudevan, et al. Searching for mobilenetv3. In *ICCV*, pages 1314–1324. IEEE, 2019. 1
- [7] Hyuck Lee and Heeyoung Kim. Cdmad: Class-distribution-mismatch-aware debiasing for class-imbalanced semi-supervised learning. In *CVPR*, pages 23891–23900. IEEE, 2024. 4
- [8] Wei Li and Xiaogang Wang. Locally aligned feature transforms across views. In *CVPR*, pages 3594–3601. IEEE, 2013. 2, 3
- [9] Wei Li, Rui Zhao, and Xiaogang Wang. Human reidentification with transferred metric learning. In *ACCV*, pages 31–44. Springer, 2012. 2, 3
- [10] Wei Li, Rui Zhao, Tong Xiao, and Xiaogang Wang. Deepreid: Deep filter pairing neural network for person re-identification. In *CVPR*, pages 152–159. IEEE, 2014. 2, 3
- [11] Chen Change Loy, Tao Xiang, and Shaogang Gong. Time-delayed correlation analysis for multi-camera activity understanding. *IJCV*, 90(1):106–129, 2010. 2, 3
- [12] Nan Pu, Wei Chen, Yu Liu, Erwin M Bakker, and Michael S Lew. Lifelong person re-identification via adaptive knowledge accumulation. In *CVPR*, pages 7897–7906. IEEE, 2021. 2, 3
- [13] Nan Pu, Zhun Zhong, Nicu Sebe, and Michael S Lew. A memorizing and generalizing framework for lifelong person re-identification. *IEEE TPAMI*, 45(11):13567–13585, 2023. 3
- [14] Jiangming Shi, Yachao Zhang, Xiangbo Yin, Yuan Xie, Zhizhong Zhang, Jianping Fan, Zhongchao Shi, and Yanyun Qu. Dual pseudo-labels interactive self-training for semi-supervised visible-infrared person re-identification. In *ICCV*, pages 11218–11228. IEEE, 2023. 4
- [15] Guanglu Song, Biao Leng, Yu Liu, Congrui Hetang, and Shaofan Cai. Region-based quality estimation network for large-scale person re-identification. In *AAAI*, 2018. 2, 3
- [16] Zhicheng Sun and Yadong Mu. Patch-based knowledge distillation for lifelong person re-identification. In *ACM MM*, pages 696–707, 2022. 4
- [17] Longhui Wei, Shiliang Zhang, Wen Gao, and Qi Tian. Person transfer gan to bridge domain gap for person re-identification. In *CVPR*, pages 79–88. IEEE, 2018. 2, 3
- [18] Ziyu Wei, Xi Yang, Nannan Wang, and Xinbo Gao. Semi-supervised learning with heterogeneous distribution consistency for visible infrared person re-identification. *IEEE TIP*, 2024. 4
- [19] Tong Xiao, Shuang Li, Bochao Wang, Liang Lin, and Xiaogang Wang. End-to-end deep learning for person search. *arXiv preprint arXiv:1604.01850*, 2(2):4, 2016. 2, 3
- [20] Kunlun Xu, Haozhuo Zhang, Yu Li, Yuxin Peng, and Jiahuan Zhou. Mitigate catastrophic remembering via continual knowledge purification for noisy lifelong person re-identification. In *ACM MM*, pages 1–9, 2024. 5

- [21] Kunlun Xu, Xu Zou, Yuxin Peng, and Jiahuan Zhou. Distribution-aware knowledge prototyping for non-exemplar lifelong person re-identification. In *CVPR*, pages 16604–16613. IEEE, 2024. [4](#), [5](#)
- [22] Kunlun Xu, Xu Zou, and Jiahuan Zhou. Lstkc: Long short-term knowledge consolidation for lifelong person re-identification. In *AAAI*, pages 16202–16210, 2024. [2](#), [4](#)
- [23] Lihe Yang, Zhen Zhao, Lei Qi, Yu Qiao, Yinghuan Shi, and Hengshuang Zhao. Shrinking class space for enhanced certainty in semi-supervised learning. In *ICCV*, pages 16187–16196, 2023. [4](#)
- [24] Haiyu Zhao, Maoqing Tian, Shuyang Sun, Jing Shao, Junjie Yan, Shuai Yi, Xiaogang Wang, and Xiaoou Tang. Spindle net: Person re-identification with human body region guided feature decomposition and fusion. In *CVPR*, pages 907–915. IEEE, 2017. [2](#), [3](#)
- [25] Liang Zheng, Liyue Shen, Lu Tian, Shengjin Wang, Jingdong Wang, and Qi Tian. Scalable person re-identification: A benchmark. In *ICCV*, pages 1116–1124. IEEE, 2015. [2](#), [3](#)
- [26] Mingkai Zheng, Shan You, Lang Huang, Chen Luo, Fei Wang, Chen Qian, and Chang Xu. Simmatchv2: Semi-supervised learning with graph consistency. In *CVPR*, pages 16432–16442. IEEE, 2023. [4](#)